PLOS COMPUTATIONAL BIOLOGY

RESEARCH ARTICLE

Coupling plankton and cholera dynamics: Insights into outbreak prediction and practical disease management

Biplab Maity[1], **Swarnendu Banerjee**[1,2,3*], **Abhishek Senapati**[1,4], **Jon Pitchford**[5,6], **Joydev Chattopadhyay**[1]

1 Agricultural and Ecological Research Unit, Indian Statistical Institute, Kolkata, India, **2** Dutch Institute for Emergent Phenomena, Institute for Biodiversity and Ecosystem Dynamics, Korteweg-de Vries Institute for Mathematics, University of Amsterdam, Amsterdam, The Netherlands, **3** Copernicus Institute of Sustainable Development, Utrecht University, Utrecht, The Netherlands, **4** Saw Swee Hock School of Public Health, National University of Singapore, Singapore, **5** Department of Biology, University of York, Wentworth Way, York, United Kingdom, **6** Department of Mathematics, University of York, Heslington, York, United Kingdom

* s.banerjee2@uva.nl

OPEN ACCESS

Citation: Maity B, Banerjee S, Senapati A, Pitchford J, Chattopadhyay J (2025) Coupling plankton and cholera dynamics: Insights into outbreak prediction and practical disease management. PLoS Comput Biol 21(9): e1013523. https://doi.org/10.1371/journal.pcbi.1013523

Editor: Claudio José Struchiner, Fundação Getúlio Vargas: Fundacao Getulio Vargas, BRAZIL

Received: April 2, 2025

Accepted: September 13, 2025

Published: September 29, 2025

Data availability statement: All data in this manuscript are generated by simulations with the MATLAB code available in the referenced GitHub repository: https://github.com/biplabmaity08/plankton_cholera.

Funding: BM is supported by Senior Research Fellowship from University Grants Commission, India (Grant no: 1220/(CSIRNETJUNE2019)).

Abstract

Despite extensive control efforts over the centuries, cholera remains a globally significant health issue. Seasonal emergence of cholera cases has been reported, particularly in the Bengal delta region, which is often synchronized with plankton blooms. This phenomenon has been widely attributed to the commensal interaction between *Vibrio cholerae* and zooplankton in aquatic environments. The role of plankton dynamics in cholera epidemiology has been acknowledged but remains poorly understood, and consequently, its importance in effective policymaking is largely overlooked. To this end, we propose and analyze a novel compartment-based transmission model that integrates phytoplankton-zooplankton interactions into a human-bacteria cholera framework. Our study shows that, beyond the reproduction number, the relative contribution of bacterial versus zooplankton-mediated transmission plays a crucial role in shaping epidemic progression and severity. In presence of zooplankton-mediated transmission, an outbreak with a delayed and lower peak may still result in a larger overall outbreak size. Additionally, contrary to common intuition, even for a large and early outbreak, the epidemic overshoot may intensify due to the maintenance of lower-level infections during the post-peak phase. Furthermore, our analysis reveals that the timing of filtration-like interventions can be strategically guided by ecological indicators, such as phytoplankton blooms. Our study underscores the importance of incorporating ecological aspects in epidemiological research to better predict and manage disease outbreaks.

Author summary

In the Bengal Delta region, cholera outbreaks re-emerge seasonally, often synchronized with plankton blooms. Although it is known that the disease is caused by *Vibrio cholerae*,

AS would like to acknowledge Senior Research Fellowship from Council of Scientific & Industrial Research, India (Grant no: 09/093(0167)/2015/EMR-I) for funding him during the initial part of this work. SB acknowledges the funding via the Foundations and Applications of Emergence (FAEME) programme at the Dutch Institute for Emergent Phenomena (DIEP), University of Amsterdam and funding via the Marie Skłodowska–Curie grant agreement 101025056 for the project 'SpatialSAVE'. The funders had no role in study design, data collection and analysis, decision to publish, or preparation of the manuscript.

Competing interests: The authors have declared that no competing interests exist.

a bacterium associated with zooplankton, the role of plankton ecology in cholera spread is not yet well understood. To address this, we have developed a novel disease transmission model that combines plankton interactions with the traditional human-bacteria cholera framework. Our findings show that when cholera spreads through zooplankton, infections can persist at a low level for a long time, leading to a large overall outbreak size, even when the number of cases at peak is not very high. The results also indicate the possibility that a large portion of the susceptible population is infected beyond the peak of infection. This underlines the need to maintain control measures during the post-peak period in regions with evidence of *Vibrio cholerae* reservoirs. We also show that not only the basic reproduction number, but also the strength of transmission pathways, plays a key role in determining the severity of an outbreak. We have also found that ecological indicators, such as phytoplankton blooms, can help to guide the timing of disease control measures like water filtration.

1. Introduction

Cholera, while treatable, remains a major global health emergency, with an estimated 4 million annual cases including 1,43,000 deaths globally [1,2]. Despite uncertainties in case reporting, recent methodologies indicate between 470,000-790,00 cholera cases, and up to 5,000 deaths, annually in the early 2020s [3,4]. The majority of these cases are in Africa, but the presence of cholera in Afghanistan, Yemen, Pakistan, Haiti, Bangladesh, and India underlines its importance in emerging and developing countries [5–9]. Country-specific factors and a critical shortage of oral vaccines in 2023 have led the WHO to categorize the resurgence of cholera as a grade 3 emergency [4].

The consistent seasonal re-emergence of cholera in the Bengal Delta region over the past decades has been attributed to seasonal plankton blooms [10–14]. It has been widely established that *Vibrio cholerae* (*V. cholerae*), the causative bacteria, is associated with plankton [15–18]. The detection of *V. cholerae* associated with zooplankton cells along the coasts of Brazil and Mexico suggests that the ecological relationship between bacteria and plankton is widespread [19,20]. Copepods, a crustacean zooplankton, are the largest known natural reservoir of the *V. cholerae* and have been implicated as a potential vector [15,21]. Experimental studies by Turner et al. [22] and Rawlings et al. [23] in natural estuarine and coastal ecosystems of Georgia, USA, as well as in the Bengal delta region found a significant correlation between *V. cholerae* density and copepod abundance. Studies indicate that a single copepod can carry 10^4 to 10^6 bacterial cells [12,24–26].

Vibrios colonize the gut of the zooplankton and the surface biofilms, where they can multiply rapidly under favorable nutrient conditions [12,18,27–29]. Further, the zooplankton protects the *Vibrios* from grazing as well as from chemical disinfectants, significantly prolonging bacterial survival compared to free-living cells [12,30–33]. This relationship between the zooplankton and the *Vibrios*, where only the former benefits from the association, is known as commensalism [18]. The empirical study by [34] asserted that, at high concentrations, *Vibrios* are more likely to attach to zooplankton cells rather than remain free in the surrounding water. As a result, exposure to commensal zooplankton could potentially lead to the consumption of a large bacterial inoculum. This underscores the fundamental role of zooplankton in cholera dynamics and emphasizes the importance of studying plankton ecology, particularly in regions with evidence of *V. cholerae* reservoirs [35].

Mathematical models have been proven to be an important and reliable tool for understanding cholera transmission mechanisms and guiding policymaking during several outbreaks [36–41]. In spite of numerous empirical studies over the past decades linking

plankton abundance to increased cholera infections [10–14,29,34,42], a mechanistic model that explicitly connects the ecology of plankton to *V. cholerae* transmission is still lacking. A recent study by Kolaye et al. [43] considered commensalism between bacteria and phytoplankton, focusing on bacterial metabolism changes. However, this study neither included any explicit compartment for commensal plankton nor studied transmission via plankton. To address this gap, we have developed a novel compartmental transmission model that integrates the phytoplankton-zooplankton interactions with the classical susceptible-infected-recovered-bacteria (SIRB) cholera model [44]. Our model includes a separate compartment for *Vibrio*-associated zooplankton cells and accounts for two transmission routes: one for free-living bacterial cells and another for bacteria-associated zooplankton. The role of zooplankton-mediated transmission in short-term epidemic outbreaks has been investigated. We assess the relative importance of transmission routes in shaping epidemic progression. Additionally, we have explored the epidemic overshoot phenomenon, which is linked to the post-peak severity of outbreaks. Further, we evaluate the effect of filtration as a practical disease management measure.

2. Methods

2.1. Model formulation

Our approach combines established SIR models for disease transmission with well-developed models for plankton dynamics, using a minimal set of biologically justifiable and quantifiable assumptions. Fig 1 and Table 1 summaries this approach. This framework facilitates a range of analyses, including the characterization of steady states and transient dynamics, computational sensitivity analysis, and the evaluation of control scenarios, across a range of ecologically relevant time scales.

The total human population at time t, $N(t)$, is divided into three compartments: susceptible ($S(t)$), infected ($I(t)$) and recovered ($R(t)$). Earlier models have typically included a single compartment for the bacterial population in the water column [44,45]. However, the commensal relationship between *V. cholerae* and zooplankton results in the bacteria being associated with zooplankton cells, which can facilitate human infection upon exposure [15,33].

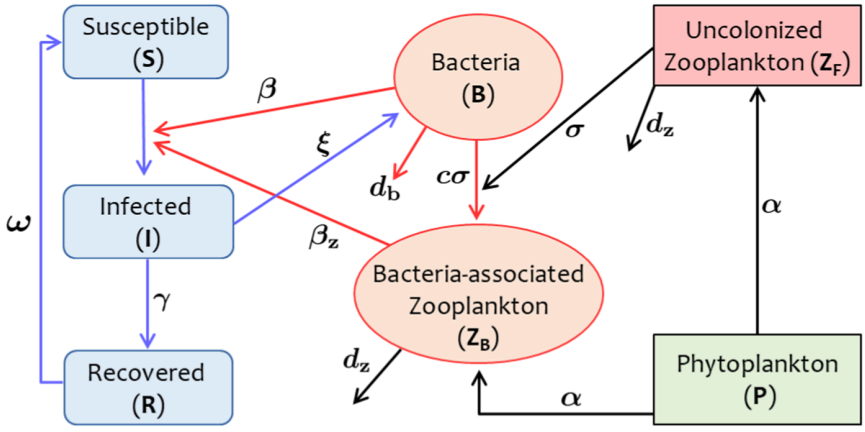

Fig 1. Coupled plankton-cholera model structure. Model schematic illustrating the linkage between phytoplankton-zooplankton interactions and the classical susceptible-infected-recovered-bacteria (SIRB) cholera model through the commensal association between *Vibrio cholerae* and zooplankton. Model parameters and their corresponding values are given in Table 1.

https://doi.org/10.1371/journal.pcbi.1013523.g001

Table 1. Description of parameters for the model (2.1).

Parameters	Description	Value	Reference
Λ	Constant recruitment rate of human population	$6.85 \times 10^{-5} \times N_0$ person day^{-1}	[49]
N_0	Initial population size	220,000	[49]
β	Transmission rate via bacteria	0.214 day^{-1}	[38,47,50]
β_z	Transmission rate via zooplankton	variable but less than β	Investigated (Sect A in S1 Text)
h_b	Half-saturation constant of bacterial transmission	10^9 cells L^{-1}	[47]
h_z	Half-saturation constant of transmission via zooplankton	20 (mg dw) L^{-1}	Investigated (Sect A in S1 Text)
μ	Natural death rate of human	3.8×10^{-5} day^{-1}	[51,52]
ω	Rate of immunity loss of recovered individuals	0.00092 day^{-1}	[49,53]
γ	Recovery rate of infected human	0.2 day^{-1}	[38,49]
δ	Disease induced mortality rate of human	0.013 day^{-1}	[36,43,50]
ξ	Bacteria shedding rate of infected humans	10-10^4 cells L^{-1} day^{-1} per person	[44,50,54]
d_b	Removal rate of the bacteria (birth - death)	0.33 day^{-1}	[43,44]
σ	Rate of bacteria-zooplankton association	0.005-0.1 day^{-1}	Investigated (Sect 3.1)
c	Colonization coefficient of bacteria	5×10^7 cells (mg dw)$^{-1}$	Investigated (Sect A in S1 Text)
h_m	Half saturation constant for bacteria-zooplankton association	10^7 cells L^{-1}	Sect A in S1 Text
η	Conversion coefficient	0.6	[55]
α	Predation rate	0.4 day–1	[55]
h_p	Half saturation constant of phytoplankton	0.6 (mg dw) L^{-1}	[55]
d_z	Death rate of zooplankton	0.06 day^{-1}	[56–58]
r_p	Growth rate of phytoplankton	0.5 day^{-1}	[55]
K	Carrying capacity of phytoplankton	0.95 (mg dw) L^{-1}	[59]

https://doi.org/10.1371/journal.pcbi.1013523.t001

This phenomenon motivates the inclusion of an explicit compartment for bacteria-associated zooplankton ($Z_B(t)$), which is formed when free-living bacteria ($B(t)$) attaches to uncolonized zooplankton ($Z_F(t)$). Hence, $Z(t) = Z_F(t) + Z_B(t)$ is the total zooplankton density at time t. The force of *Vibrio*-zooplankton commensalism is represented by the term $c\sigma\frac{B}{h_m + B}$. Here, σ denotes the rate of bacteria-zooplankton association and h_m is the half-saturation constant of the association. The parameter c represents the average number of *Vibrio* cells per zooplankton, which we term the 'colonization coefficient'. Since phytoplankton ($P(t)$) governs zooplankton ($Z(t)$) abundance, we consider the dynamics of phytoplankton-zooplankton using a well-studied Rosenzweig–MacArthur type model [46].

Susceptible humans become infected through exposure to free-living bacteria (via water contamination), $B(t)$, with a force of infection $\lambda_B = \frac{\beta B}{h_b + B}$ and *Vibrio*-associated zooplankton, $Z_B(t)$, with a force of infection $\lambda_Z = \frac{\beta_z Z_B}{h_z + Z_B}$. Here, h_b and h_z represent the half-saturation

constant for transmission via bacterial and zooplankton routes, respectively. Note that h_z depends on the pathogen load of commensal zooplankton and is inversely proportional to the bacterial colonization coefficient, c. The use of Holling type-II transmission terms follows existing literature [44,45,47]. Our model, which includes transmission via both free-living bacteria and bacteria-associated zooplankton, is given as follows (see Fig 1 for schematic).

$$\begin{aligned}
\frac{dS}{dt} &= \Lambda - \frac{\beta SB}{h_b + B} - \frac{\beta_z S Z_B}{h_z + Z_B} - \mu S + \omega R,\\
\frac{dI}{dt} &= \frac{\beta SB}{h_b + B} + \frac{\beta_z S Z_B}{h_z + Z_B} - (\gamma + \mu + \delta) I,\\
\frac{dR}{dt} &= \gamma I - (\mu + \omega) R,\\
\frac{dB}{dt} &= \xi I - d_b B - c\sigma \frac{B Z_F}{h_m + B},\\
\frac{dZ_B}{dt} &= \sigma \frac{B Z_F}{h_m + B} - d_z Z_B,\\
\frac{dZ_F}{dt} &= \eta \frac{\alpha P (Z_F + Z_B)}{h_p + P} - d_z Z_F - \sigma \frac{B Z_F}{h_m + B},\\
\frac{dP}{dt} &= r_p P\left(1 - \frac{P}{K}\right) - \frac{\alpha P (Z_F + Z_B)}{h_p + P}.
\end{aligned} \tag{2.1}$$

Infected individuals either recover at a rate γ or die due to infection at a rate δ and contribute bacterial cells into the environment through excretion at a rate ξ over their infectious period. As cholera does not confer life-long immunity [45,48], recovered individuals, although initially immune to the pathogen, eventually lose immunity at a rate ω and replenish into the susceptible compartment. Λ denotes the recruitment rate of susceptible individuals through birth and immigration, while each class experiences a natural death rate μ. Here, d_b represents the rate of loss of free-living bacteria, accounting for both mortality and the decline in vitality. Phytoplankton grows at a rate r_p up to its maximum achievable density, known as the carrying capacity, K. The maximal grazing rate of the zooplankton on phytoplankton is α with a conversion coefficient η. Here, d_z and h_p refer to the zooplankton death rate and the half-saturation concentration of zooplankton grazing, respectively.

Note that the plankton dynamics, represented by the last three equations in model (2.1), is independent of the human-bacteria (SIRB) dynamics (see Sect C in S1 Text). This independence implies that the bacteria-zooplankton association does not influence overall plankton density, which is representative of the commensal interaction. However, this association leads to the formation of Z_B and reduces free-living bacterial density, thereby affecting human-bacteria dynamics. Note that we do not consider direct human-to-human transmission here, as it has been shown that the aquatic environment plays a decisive role in the survival and transmission of pathogens during cholera outbreaks in several regions [15]. If the bacteria-zooplankton association is excluded (i.e. $\sigma = 0$), our model (2.1) resembles previous SIRB cholera models, such as those used in [44,48].

3. Results

Our results are presented according to the ecologically and management-motivated time scales relevant to this study. The main body of work (Sect 3.1) analyses cholera outbreaks in

human populations over a short time scale, where human population and immunity dynamics can be neglected (i.e. $\mu, \Lambda = 0$ and $\omega = 0$ in model (2.1)). We then contextualize these findings in the context of practical interventions connected to water filtration (Sect 3.2).

3.1. Outbreak dynamics

To remove the effect of transient plankton dynamics on disease outbreak, we consider the coexistent steady-state plankton densities as the initial condition for phytoplankton ($P_0 = P^*$) and zooplankton ($Z_{F_0} = Z^*, Z_B = 0$) in model (2.1) (see Sect C in S1 Text for P^*, Z^*). This approach is reasonable in light of the following: (i) the transient plankton dynamics has no biological significance in the context of an outbreak, and (ii) the outbreak does not alter the plankton dynamics. Note that the zooplankton-free equilibrium ($Z_F = Z_B = 0$) of the phytoplankton-zooplankton system is not relevant in the context of our study.

The necessary condition for the initial growth of an outbreak in the presence of both transmission routes is given by (see Sect D in S1 Text)

$$\begin{aligned}\mathcal{R}_{0_{\mathrm{BZ}}}^{\mathrm{out}} &= \mathcal{R}_{0_B}^{\mathrm{out}} + \mathcal{R}_{0_Z}^{\mathrm{out}} \\ &= \frac{\xi N_0}{(\gamma+\delta)\left(d_b + c\sigma\frac{Z^*}{h_m}\right)}\left[\frac{\beta}{h_b} + \frac{\beta_z}{h_z}\sigma\frac{Z^*}{d_z h_m}\right] > 1 \end{aligned} \tag{3.1}$$

where

$$\begin{aligned}\mathcal{R}_{0_B}^{\mathrm{out}} &= \frac{\xi N_0}{(\gamma+\delta)\left(d_b + c\sigma\frac{Z^*}{h_m}\right)}\frac{\beta}{h_b}, \\ \mathcal{R}_{0_Z}^{\mathrm{out}} &= \frac{\xi N_0}{(\gamma+\delta)\left(d_b + c\sigma\frac{Z^*}{h_m}\right)}\frac{\beta_z}{h_z}\sigma\frac{Z^*}{d_z h_m}.\end{aligned}$$

Here, $\mathcal{R}_{0_{\mathrm{BZ}}}^{\mathrm{out}}$ denotes the basic reproduction number (see Sect E in S1 Text for the basic reproduction number in the long-term scenario). Also, $\mathcal{R}_{0_B}^{\mathrm{out}}$ and $\mathcal{R}_{0_Z}^{\mathrm{out}}$ represent contributions associated with the free-living bacterial route and the bacteria-associated zooplankton route, respectively, to the initial outbreak growth.

3.1.1. Impact of bacteria-zooplankton association on $\mathcal{R}_{0_{\mathrm{BZ}}}^{\mathrm{out}}$. In the absence of the bacteria-zooplankton (B-Z) association (i.e. $\sigma = 0$), the condition for the initial outbreak growth $\mathcal{R}_0^{\mathrm{out}} = \mathcal{R}_{0_{\mathrm{BZ}}}^{\mathrm{out}}|_{\sigma=0} = \frac{\xi N_0}{d_b(\gamma+\delta)}\frac{\beta}{h_b} > 1$, aligns with the classic SIRB cholera model [44]. The colonization of zooplankton by bacterial cells reduces the free-living bacterial density, thereby lowering $\mathcal{R}_{0_B}^{\mathrm{out}}$. This association simultaneously increases $\mathcal{R}_{0_Z}^{\mathrm{out}}$ through the transmission via commensal zooplankton. As a result, for a specific β, the B-Z association can lead to an increase or decrease of $\mathcal{R}_{0_{\mathrm{BZ}}}^{\mathrm{out}}$ relative to $\mathcal{R}_0^{\mathrm{out}}$ depending on σ and β_z.

The two-parameter space (β-β_z) can be divided into six regions using the three lines, $\mathcal{R}_0^{\mathrm{out}} = 1$ (dashed vertical line), $\mathcal{R}_{0_{\mathrm{BZ}}}^{\mathrm{out}} = 1$ (red line), and $\mathcal{R}_{0_{\mathrm{BZ}}}^{\mathrm{out}} = \mathcal{R}_0^{\mathrm{out}}$ (black line) (Fig 2A). While, in region 1 and 6, the B-Z association increases $\mathcal{R}_{0_{\mathrm{BZ}}}^{\mathrm{out}}$ compared to $\mathcal{R}_0^{\mathrm{out}}$, in 2 and 3, it decreases the same. Here, the decrease in $\mathcal{R}_{0_{\mathrm{BZ}}}^{\mathrm{out}}$ can be achieved with reduced β_z, which signifies the reduced exposure to zooplankton contaminated water. It is interesting to note that in 6, an outbreak cannot initiate without the B-Z association, highlighting the significance of zooplankton-driven route. This contrasts with the behavior in 3, where an

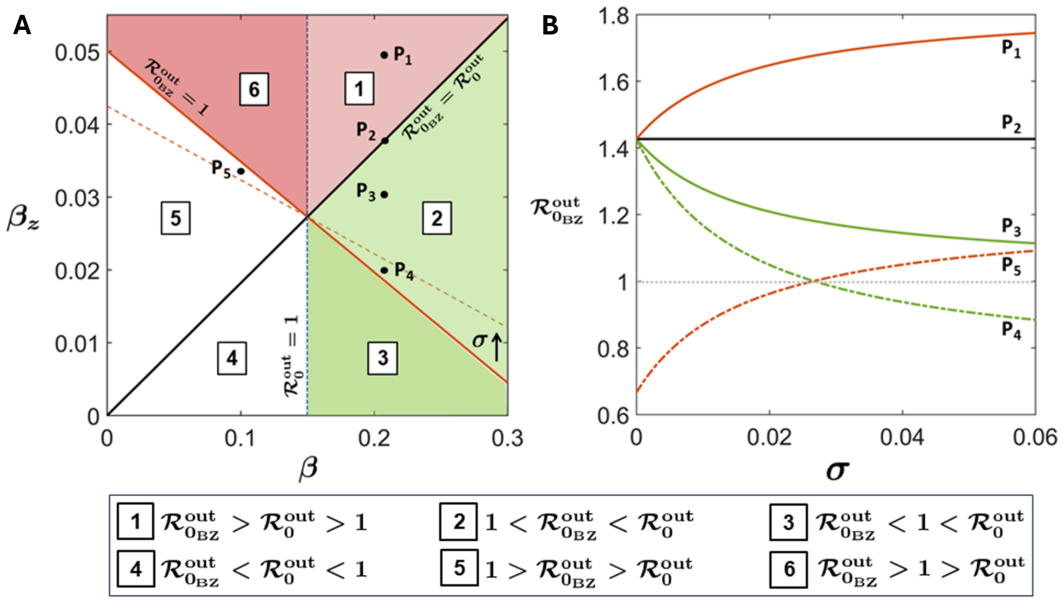

Fig 2. Impact of bacteria-zooplankton association on $\mathcal{R}^{out}_{0BZ}$. (A) Effect of the transmission rates β, β_z. The red and black lines depict $\mathcal{R}^{out}_{0BZ} = 1$ and $\mathcal{R}^{out}_{0BZ} = \mathcal{R}^{out}_{0}$, respectively. The vertical dashed line indicates $\mathcal{R}^{out}_{0} = 1$, corresponding to the absence of the *B*-*Z* association. An increase in σ expands regions [6] and [3] at the expense of [5] and [2], respectively, as indicated by the red-dashed line. (B) The effect of the association rate (σ) on points P_1-P_5, which belong to different regions demonstrated in (A).

https://doi.org/10.1371/journal.pcbi.1013523.g002

outbreak that can grow without this association decays in its presence. In regions [4] and [5], the outbreak fails to grow irrespective of the presence or absence of the *B*-*Z* association, making it insignificant in the context of our study. For a lower β, a relatively high β_z can still trigger an outbreak when $\mathcal{R}^{out}_{0BZ} > 1$. This implies that zooplankton-mediated transmission can compensate for a low transmission rate via free-living bacteria.

For any point in [1], e.g. P_1, an increased bacteria-zooplankton association rate (σ) always increases $\mathcal{R}^{out}_{0BZ}$ (red line Fig 2B). Further, slope of the line $\mathcal{R}^{out}_{0BZ} = 1$ decreases with increasing σ (red-dashed line in Fig 2A) (see Sect D in S1 Text for details). As a result, regions [3] and [6] expand at the expense of [2] and [5], respectively. Consequence of this can be observed by following the fate of the outbreak on increasing σ at points P_4 and P_5. At P_4, where the outbreak initially grows ($\mathcal{R}^{out}_{0BZ} > 1$), the system is driven to the region where the outbreak decays ($\mathcal{R}^{out}_{0BZ} < 1$) with increasing σ (green-dashed line in Fig 2B). The converse is true for the point P_5 as shown by red-dashed line in Fig 2B. Additionally, there are some points in [2], e.g. P_3, for which increasing σ will decrease $\mathcal{R}^{out}_{0BZ}$ while still maintaining it above 1 (green line in Fig 2B). The black (P_2) line in Fig 2B represents the scenario $\mathcal{R}^{out}_{0BZ} = \mathcal{R}^{out}_{0}$ under any association rate (σ). Moreover, from Fig 2B, it is important to note that for a fixed β, changes in β_z (e.g., P_1-P_4) lead to relatively larger variations in $\mathcal{R}^{out}_{0BZ}$ under a high σ compared to a lower one. This can be explained by the fact that under favorable conditions, large number of *Vibrio*-associated zooplankton cells significantly impact the disease spread. We use global sensitivity analysis to show that the above result holds true for all values of β (see Sect D in S1 Text).

Notably, in this study, we always consider $d_z < d_b$, which is well supported by ecological evidences [43,44,56–58]. An increase in d_z increases the slope of the $\mathcal{R}^{out}_{0BZ} = \mathcal{R}^{out}_{0}$ line,

thereby reducing the region $\boxed{1}$ (see S1 Fig). This indicates a diminished effect of transmission via zooplankton as the persistence of bacterial cells in association with zooplankton is reduced.

3.1.2. Relative contribution of transmission routes. The ratio of contributions to the basic reproduction number ($\mathcal{R}_{0_{BZ}}^{out}$) from zooplankton ($Z_B$) and bacterial ($B$) routes can be expressed as $\mathcal{R}_{0_Z}^{out}/\mathcal{R}_{0_B}^{out} = (\sigma Z^* h_b \beta_z)/(d_Z h_z h_m \beta)$. Environmental factors, such as fluctuations in the temperature of the coastal sea surface, salinity, pH, heatwave, rainfall, floods, and ecological events such as plankton blooms, can influence the bacteria-zooplankton association [28,30,60], causing one transmission route to become more prominent over the other. Therefore, it is crucial to investigate for a fixed $\mathcal{R}_{0_{BZ}}^{out}$, how altering relative contributions ($\mathcal{R}_{0_B}^{out}$, $\mathcal{R}_{0_Z}^{out}$) through different transmission routes can impact disease progression and overall disease burden. To this aim, we keep $\mathcal{R}_{0_{BZ}}^{out} = \mathcal{R}_0^{out} > 1$, which always implies $\beta_z = \frac{ch_z d_z}{h_b d_b}\beta$ (black line in Fig 2A). For a fixed β, corresponding to each pair of relative contributions ($\mathcal{R}_{0_B}^{out}$, $\mathcal{R}_{0_Z}^{out}$), the unique association rate σ is given by (see Sect D in S1 Text for details)

$$\sigma = \frac{d_b h_m}{cZ^*}\left(\frac{\mathcal{R}_{0_{BZ}}^{out}}{\mathcal{R}_{0_B}^{out}} - 1\right) = \frac{d_b h_m}{cZ^*}\frac{\mathcal{R}_{0_Z}^{out}}{\mathcal{R}_{0_B}^{out}}.$$

Now, we compare outbreak trajectories by varying σ that captures scenarios for different relative contributions from the both routes. We examine various characteristics of these trajectories such as peak values, peak timing, cumulative infections, and epidemic duration (see Fig 3).

In the absence of *Vibrio*-zooplankton association ($\sigma = 0$), transmission only via the bacterial route drives the prevalence with a relatively higher and earlier peak, followed by a steeper decline (black line in Fig 3A). When the Z_B route contributes a moderate to high proportion (20% to 60%), the outbreak progresses over a longer duration with delayed and reduced epidemic peak (Fig 3A and 3D). However, it results in a slightly increased proportion of cumulative infections both at peak and at the end of the outbreak, compared to the $\sigma = 0$ scenario (Fig 3B). The delayed dynamics in the presence of the B-Z association arise because the contribution from the Z_B route leads to a comparatively slower initial epidemic growth rate (EGR) (Fig 3D and Sect D in S1 Text for EGR calculations). The zooplankton-mediated transmission route can be viewed as a delayed transmission pathway, as the zooplankton have to first be colonized by bacteria cells before transmitting the infection to susceptible persons. The increase in cumulative infections at the peak in the presence of the zooplankton route means greater depletion of susceptible population before the peak and indicates an increased threshold of herd immunity for the same $\mathcal{R}_{0_{BZ}}^{out}$ (Fig 3B). These observations emphasize that predictions about the outbreak trajectories and disease severity can not be precisely determined only by analyzing $\mathcal{R}_{0_{BZ}}^{out}$, the contribution of transmission routes is also important.

In spite of the increasing cumulative infections, the Z_B route produces fewer new infections compared to the B route in each case (Fig 3B and 3C). In fact, the epidemic peak's size and timing are primarily determined by the B route, which is responsible for the majority of new infections (Fig 3C). Increasing $\mathcal{R}_{0_Z}^{out}$ leads to reduced density of B cells which results in a lower peak of infections. This occurs because, when $\mathcal{R}_{0_{BZ}}^{out} = \mathcal{R}_0^{out}$, (i.e. $\beta_z = \frac{ch_z d_z}{h_b d_b}\beta$, black line in Fig 2A), we always have $\beta_z < \beta$ as $d_z < d_b$ and thus, the Z_B route always provides a lower force of infection than the B route.

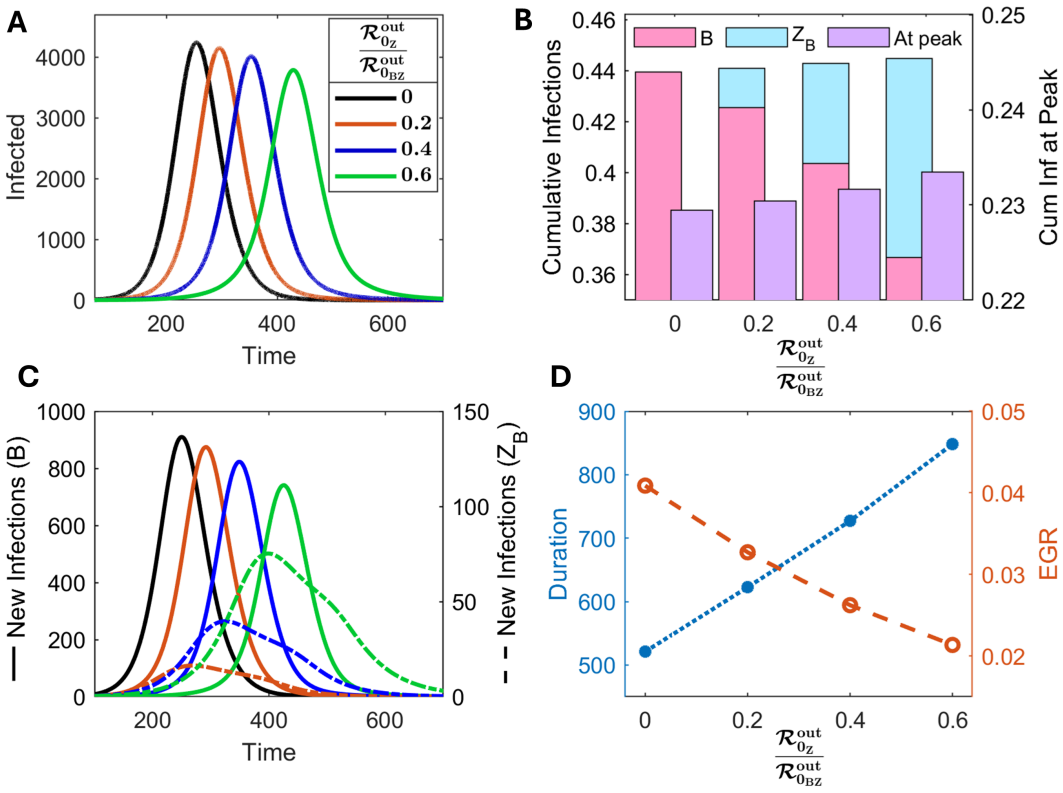

Fig 3. Effect of changing the relative contribution of transmission routes while keeping $\mathcal{R}_{0_{BZ}}^{out}$ fixed. (A) Active infections, (B) cumulative infections (proportion of the population), (C) new infections via the B (solid lines) and Z_B (dashed lines) route, and (D) epidemic duration (blue dotted) and initial epidemic growth rate (EGR) (red dashed). Increasing $\mathcal{R}_{0_Z}^{out}$ decreases initial EGR, delays and lowers the peak, but increases cumulative infections both at the peak and at the end of the outbreak.

https://doi.org/10.1371/journal.pcbi.1013523.g003

3.1.3. Nature of outbreak trajectories. In this section, we investigate the nature of the outbreak trajectories within region 1 of Fig 2A while varying the bacteria-zooplankton association rate (σ) for different zooplankton-mediated transmission rate (β_z). For high $\beta_z = 0.08$, an increased σ leads to both earlier (EGR increases) and higher peaks compared to $\sigma = 0$ case (Fig 4B, 4C, 4E and S2 Fig). When β_z is low ($\beta_z = 0.04$), a delayed and lower peak is observed. However, for intermediate β_z (=0.05), while the peak is delayed, the number of infections at peak increases (Fig 4B, 4C, 4F and 4G). The decrease in EGR with increasing σ for both $\beta_z = 0.04$ and $\beta_z = 0.05$ explains the delayed dynamics in these scenarios (see S2 Fig). Since an outbreak with a delayed and lower peak can still result in a larger outbreak size (due to higher $\mathcal{R}_{0_{BZ}}^{out}$ at increased σ, Fig 4A), it may not be easy to predict the outbreak size based on peak value and peak timing when zooplankton-mediated transmission is involved (Fig 4G). For all of the above scenarios, the epidemic duration increases noticeably, compared to the $\sigma = 0$ case (Fig 4D).

Under fixed $\sigma = 0.03$, an increased β_z leads to an increased duration of epidemic in spite of earlier and larger peak value (Fig 4 and S3 Fig). This is due to the fact that increasing β_z results in a considerably slower asymptotic convergence of the infection trajectory to the disease-free state after the peak infections, thus prolonging the duration of the outbreak (for example, see Fig 4E). This is in contrary to the usual notion whereby an epidemic trajectory

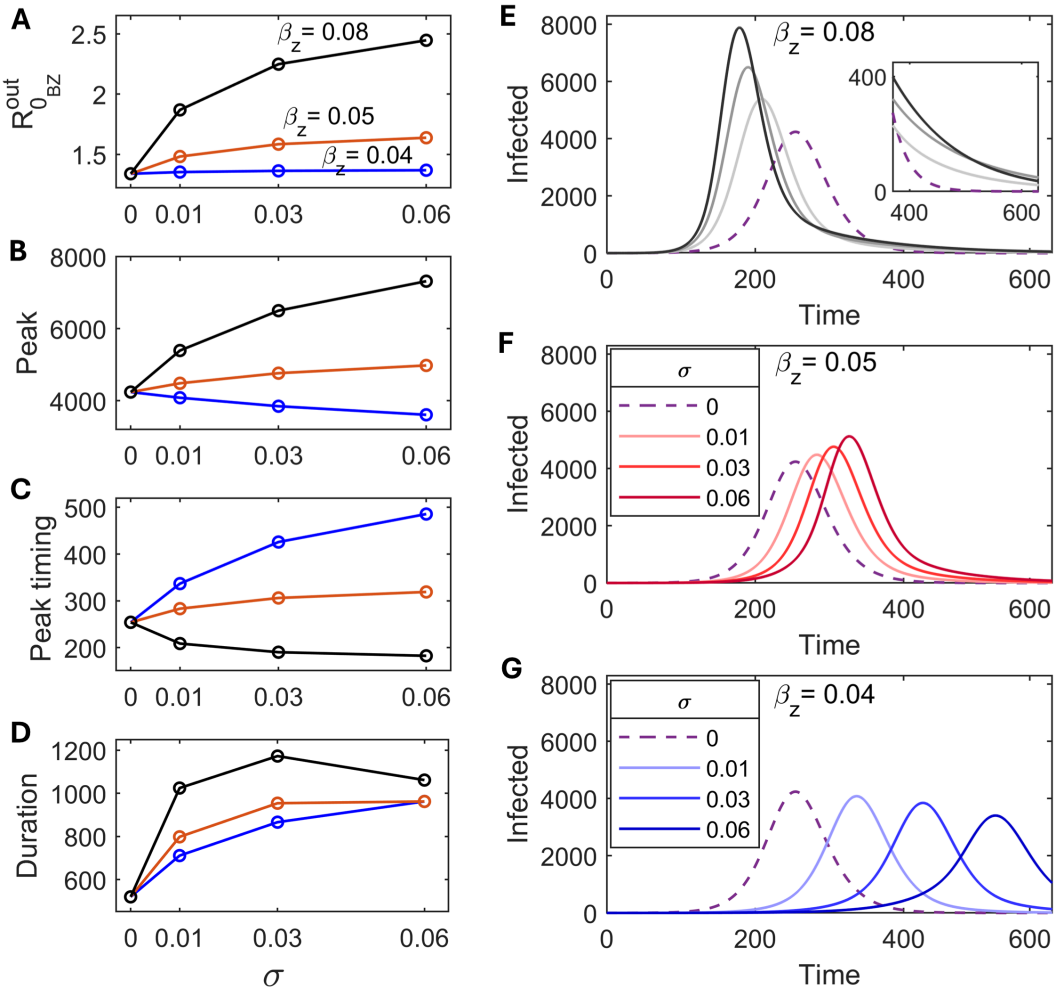

Fig 4. Influence of association rate and zooplankton-mediated transmission on epidemic dynamics. $\mathcal{R}^{out}_{0_{BZ}}$ (A), peak infections (B), peak timing (C), epidemic duration (D) and the outbreak trajectories (E-G) under varying bacteria-zooplankton association rate (σ) for different transmission rates via zooplankton (β_z) within region 1 of Fig 2A.

https://doi.org/10.1371/journal.pcbi.1013523.g004

with a higher reproduction number should results in a relatively larger and faster peak followed by a quicker decline. This observation underscores the importance of zooplankton in promoting pathogen persistence during inter-epidemic periods by serving as a *V. cholerae* reservoir. The maintenance of lower-level infections for a long period continues to influence the number of infections after the peak or equivalently after achieving the herd immunity threshold. In this context, the next subsection explores the epidemic overshoot phenomenon, which accounts for outbreak severity in the post-peak phase.

3.1.4. Epidemic overshoot. Epidemic overshoot refers to the proportion of the population that becomes infected after the peak of infection has passed, i.e. during the post-peak phase. It is equivalent to the difference between the herd immunity threshold and the attack rate (i.e. proportion of the infected population) [61]. Notably, the ratio of overshoot to attack rate (ρ_{OA}) is an important metric for quantifying the fraction of total infections occurring at the overshoot phase [62]. In the absence of bacteria-zooplankton association ($\sigma = 0$), in line with a simple SIR system, higher transmission rates from the free-living bacterial route (β)

always burn a significant portion of the population before reaching peak prevalence, leading to a sharp rise in infections and leaving fewer susceptible individuals for the overshoot phase. As a result, the ratio of overshoot to attack rate (ρ_{OA}) decreases monotonically as β increases in case of $\sigma = 0$ (see S4 Fig).

In presence of bacteria-zooplankton association ($\sigma \neq 0$), increasing transmission via zooplankton (β_z) for a fixed β alters the above observations. We find that, along with cumulative infections at the peak and the attack rate, the overshoot also increases substantially across a wide range of β_z (see Fig 5A and 5B). Interestingly, it appears that the increase in the overshoot due to β_z profoundly surpasses the rise in cumulative infections at the peak (solid red and blue line Fig 5B). For instance, 50% increase in $\beta_z = 0.05$ results in 7% and 30% increase in cumulative infections at peak and the overshoot, respectively (Fig 5B). Consequently, the ratio of overshoot to attack rate (ρ_{OA}) increases significantly over a wide range of β_z, which is contrary to what is usually observed in SIR systems (see Fig 5C). This result is particularly interesting, indicating a substantial overshoot in cases where transmission via zooplankton is more pronounced. Therefore, alongside transmission from the free-living bacterial route, even moderate transmission via zooplankton infects a larger portion of the susceptible population in the post-peak phase by sustaining lower-level infections over an extended period

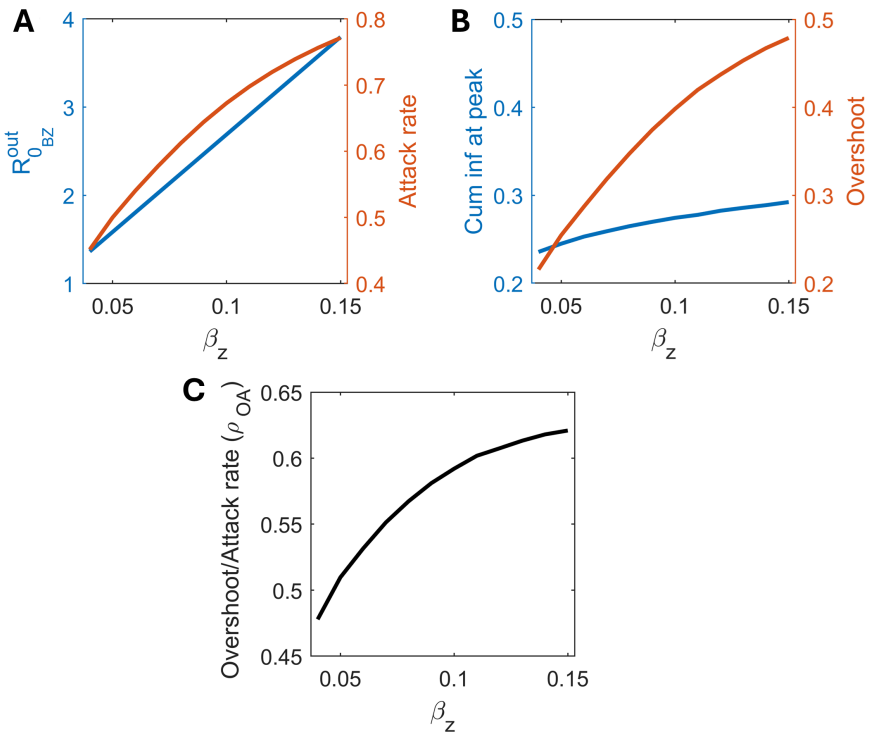

Fig 5. Influence of zooplankton-mediated transmission on epidemic overshoot. Effect of on (A) $\mathcal{R}^{out}_{0_{BZ}}$ and attack rate, (B) cumulative infections at peak (as proportion of the total population) and overshoot, and (C) ratio of overshoot to attack rate (ρ_{OA}). Parameter: $\sigma = 0.03$.

https://doi.org/10.1371/journal.pcbi.1013523.g005

before eventually fading out. This underscores that maintenance of control measures during the post-peak phase becomes crucial to prevent additional overshoot. It should be noted that extremely large β_z values (for which $\mathcal{R}_{0_{BZ}}^{out}$ may not be feasible for cholera (Eq. (3.1))) cause both the overshoot and ρ_{OA} to decline again (not shown here).

3.2. Disease management via water filtration

In the Bengal delta region, numerous studies have documented seasonal fluctuations in *Vibrio* cells attached to zooplankton, with the highest concentrations observed during the early spring and summer, coinciding with the peak zooplankton populations [11,13,14,60]. We note that our model, by explicitly considering the various ecological time scales involved, presents an opportunity to incorporate seasonality and its connection to disease dynamics and potential control measures. To qualitatively mimic the emergence of cholera infections preceded by biannual plankton blooms, we consider the phytoplankton carrying capacity (K) to be a periodic function given by

$$K(t) = K_0(1 + d\sin(2\pi t/p)).$$

Here K_0 stands for the baseline phytoplankton carrying capacity, while d and p denote the amplitude and period of oscillation, respectively. This assumption is reasonable as the carrying capacity depends on fluctuations in climatic and environmental factors such as coastal sea surface temperature, nutrient load, salinity, pH, flooding and streamflow [43–45,59,60,63,64]. Note that we ensure $K(t)$ remains below the critical carrying capacity K^c, beyond which the plankton system no longer shows stable coexistence (see Sect C in S1 Text). In this case, we also consider human demographic and immunity factors ($\Lambda, \mu, \omega \neq 0$).

The copepod-associated *Vibrio cholerae* cells remains viable even after treatment of household water with chemical disinfectants like alum and chlorination [31]. However, a sari cloth folded four times can remove up to 99% bacteria-associated zooplankton cells, as demonstrated in the laboratory-based study by Huq et al. [65]. Furthermore, an experimental study conducted in Matlab, Bangladesh, by Colwell et al. [66] found that filtration using simple sari and nylon cloths can remove around 90% of bacteria cells attached to copepods. Hence simple filtration of household water can be a more effective method of controlling cholera compared to chemical-based purification. This is particularly relevant in adverse situations including humanitarian crises and climate-driven extreme weather events, where access to clean water is limited, making an inexpensive, easy-to-use, and socially acceptable household water treatment method like filtration essential [3,67]. Additionally, the waning of vaccine-induced immunity, combined with the ongoing critical shortage of oral vaccines (OCV) further reinforces the need for household control measures [4,68].

Filtration is a point-of-use (POU) water purification method, typically applied when collecting water from reservoirs such as lakes and ponds [66,69,70]. By removing planktonic organisms, filtration effectively reduces zooplankton concentration and thus the infectious dose in household water [37,69]. This, in turn, directly impacts the force of infection via the zooplankton-driven transmission route. Other POU measures, such as boiling and household chlorination [71], are not considered here, as our focus is on assessing the impact of controlling infection through the zooplankton-mediated route. To model filtration, we modified the zooplankton-driven force of infection term as follows:

$$FI_Z(t) = \begin{cases} \beta_z \dfrac{(1-e_f)Z_B(t)}{h_z + (1-e_f)Z_B(t)}, & \text{during filtration} \\ \beta_z \dfrac{Z_B(t)}{h_z + Z_B(t)} & \text{else.} \end{cases} \tag{3.2}$$

Here e_f stands as the filtration efficacy, which quantifies the proportion of dispelled zooplankton cells and depends on the procedure's accuracy and the mesh size of the used material. For instance, sari cloths appeared to be more effective than nylon nets in removing copepods [66]. Note that we assume an instantaneous effect of filtration on $FI_Z(t)$, which is reasonable as the water is typically collected on a daily basis for household use.

An important question is when to initiate filtration and how long the control measure should last. Notably, plankton blooms typically serve as an early warning indicator for cholera outbreaks, with a lag of nearly 8 weeks between plankton blooms and the rise in cholera infections, as observed in the Bengal Delta region [13,24]. So, one can think of two indicators for initiation of filtration: the occurrence of phytoplankton blooms, which are mostly recognizable in water reservoirs, and an increase in cholera infections. Since plankton blooms generally last for about three months, we focus on implementing periodic filtration with same duration. We assess the outcome of filtration by measuring the reduction in the number of infections over a year, compared to the situation without filtration. Implementing filtration measures based on the two indicators implies different initiation times, which may lead to differences in cholera case reduction. We also analyze the impact of filtration initiated at all time points, while maintaining the same duration as above for each case.

The overall effect of filtration on reducing cholera infection at different initiation timings is illustrated in Fig 6. The solid line in Fig 6A indicates the percentage reduction in cholera infections associated with different filtration initiation timings (dashed vertical lines). Fig 6B depicts two filtration indicators: the phytoplankton density (solid black line) and the subsequent rise in infections (red line), alongside zooplankton abundance (dotted black line). Four different filtration initiation timings, T_1-T_4 are considered among which T_1 and T_3 follow the former and the latter indicator, respectively (Fig 6A and 6B). Additionally, the active and cumulative infections under filtration corresponding to timings T_1-T_4, along with the unfiltered scenario, are shown in Fig 6C–6F, respectively. We observe that, when filtration is employed with an efficacy of 80% (i.e. $e_f = 0.8$), the reduction in cholera infections varies from approximately 32% to 65%, depending on the timing of initiation (Fig 6A). Filtration initiated at T_1 following a phytoplankton bloom reduces around 50% infections (Fig 6C), which is slightly less effective than the 54% reduction observed when filtration is initiated at T_3 in response to increasing cholera infections (Fig 6E).

The above results can be explained by tracking the formation and ingestion of Z_B in our simulations. Filtration initiated at T_1 ends when Z abundance is close to its peak, leading to considerable formation of Z_B which are then ingested (Figs 6C and S5A). On the other hand, when filtration is initiated at T_3, in spite of significant Z_B formation, it can lead to relatively less ingestion during the high abundance period (Figs 6E and S5C). Filtration initiated at T_2, which continues during periods of high Z abundance, effectively restricts both formation and ingestion of Z_B, appears to be the best-case scenario (Figs 6D and S5B). Hence, in this case, infections remain relatively low throughout the year (nearly 65% reduction in Fig 6(D)). This indicates that initiating filtration during rising zooplankton abundance (T_2), rather than in response to rising infections (T_3), leads to comparatively greater reduction in infection.

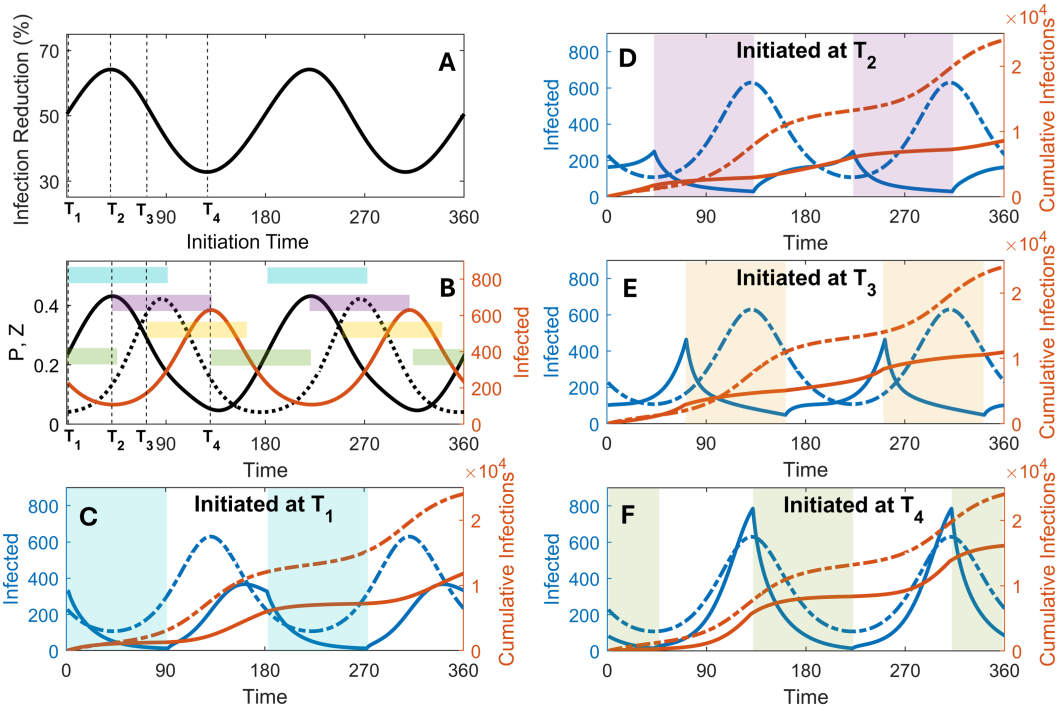

Fig 6. Effect of 90-day periodic filtration on reducing cholera infections linked to seasonal biannual plankton blooms. (A) the percentage of infection reduction (solid line) over a year for different initiation timings. Here T_1-T_4 represents four distinct initiation timings. (B) Illustrates potential indicators for initiating filtration, based on increase in phytoplankton density over time (solid black line) and subsequent increases in infections (red line) along with the zooplankton abundance (dotted black line). The scenario when filtration is initiated at T_1 following the phytoplankton bloom (C), at T_2 when zooplankton abundance is increasing (D) (best-case scenario), at T_3 in response to an increasing trend in infections (E) and at T_4 when delayed until near the infection peak (F) (worst-case scenario). In (C)-(F), active (blue) and cumulative (red) infections are shown for both filtered (solid lines) and unfiltered (dashed lines) scenarios. The shaded regions indicate the filtration periods. Here we consider filtration with 80% efficacy (i.e. $e_f = 0.8$) and $K(t)$ is parameterized by $d = 0.8$ and $K_0 = 0.27$.

https://doi.org/10.1371/journal.pcbi.1013523.g006

The worst-case scenario arises from delayed filtration initiated near the infection peak at T_4, which fails to restrict both formation and ingestion of Z_B (S5D Fig). In this case, a rapid peak, even larger than the uncontrolled one arises although with a reduced total infection over the year (nearly 32% reduction in Fig 6F). Moreover, infection reduction increases with filtration efficacy, with incremental reduction becoming more pronounced at higher efficacy levels (see S6 Fig and Sect E in S1 Text). Overall, these observations underscore the importance of timely and accurate filtration practices for reducing cholera infections.

4. Discussion

Cholera remains a reemerging disease of poverty for nearly 2 billion people in over 50 countries who have inadequate access to safe water and poor sanitation infrastructure [7]. Despite the well-documented correlation between plankton blooms and cholera outbreaks over the past decades, the impact of plankton ecology on cholera dynamics has not yet been fully explored from a mathematical modeling perspective. To this aim, we integrate phytoplankton-zooplankton interactions into the classical human-bacteria (SIRB) cholera model through the ecological commensal association between *V. cholerae* and zooplankton. This could lead different dynamics of cholera outbreak which has remain unexplored until now. For instance,

an outbreak that might initially decay without the bacteria-zooplankton association can grow when the transmission via zooplankton is involved. On the other hand, this association can also lead to decline in initial infections which would have grown otherwise. Additionally, there will be scenarios where transmission via zooplankton increases the spread of the disease, i.e., $\mathcal{R}_{0_{BZ}}^{out}$ (Fig 2).

The basic reproduction number ($\mathcal{R}_{0_{BZ}}^{out}$) alone may not provide complete picture about outbreak trajectories or disease severity. The relative contribution of transmission routes, influenced by ecological, environmental, and climatic factors, plays a significant role in determining the progression and impact of an outbreak (Fig 3). Although the zooplankton route is responsible for fewer infections compared to the free-living bacterial route, the outbreak persists longer in the presence of bacteria-associated zooplankton cells. The colonization of zooplankton by *V. cholerae* cells prior to human exposure makes the zooplankton route a delayed transmission pathway. This is consistent with the the results of [72]. For a fixed reproduction number, the dominant free-living bacterial route drives rapid outbreak growth with a higher peak. In contrast, even moderate transmission via the zooplankton route results in a comparatively slower outbreak progression with a reduced peak. However, this leads to a higher herd immunity threshold, larger final size, and longer outbreak duration. This finding aligns with the contrasting epidemiological patterns of cholera: the Ganges delta region experiences consistent, longer outbreaks involving reservoir transmission, while the African region often reports shorter, sporadic outbreaks without reservoir transmission, as noted by Sack et al. [73]. This result emphasizes the consideration of relative contributions of transmission routes while designing interventions. Also, it underscores the importance of maintaining control measures despite a slower initial growth of the outbreak, particularly in regions with evidence of *V. cholerae* reservoirs.

Even when the basic reproduction number ($\mathcal{R}_{0_{BZ}}^{out}$) increases due to zooplankton-mediated transmission, we can observe both an early or a delayed peak, depending on the different rates of the bacteria-zooplankton association. While the former is the usual expectation, the latter is unintuitive. However, in both cases, a larger outbreak size is reached due to prolonged infections at lower levels during the post-peak phase (Fig 4). This highlights the role of environmental reservoirs in prompting the inter-epidemic persistence of pathogens, as noted in previous studies [15,18,73]. In fact, the increase in overshoot may surpass the rise in cumulative infections at the peak when the transmission rate via zooplankton increases (Fig 5). This contrasts with classical SIR systems, in which the ratio of overshoot to attack rate declines monotonically as transmission increases [62]. This finding highlights the possibility of substantial overshoot in regions with the evidence of *V. cholerae* reservoirs, such as the Ganges delta region, and underscores the need to maintain control measures during the post-peak period. Relaxing control measures beyond the peak of infections, even after achieving herd immunity, could potentially lead to additional overshoot.

Lastly, we also study disease management via practical control measure such as water filtration, which has previously been deemed effective to reduce cholera in endemic regions like Matlab, Bangladesh [66]. Our findings indicate that the timing of implementing such a control measure can be a key to a substantial (approximately 32 – 65%) reduction in cholera infections (Fig 6). Initiating filtration during rising zooplankton abundance yields the greatest infection reductions, underscoring the importance of ecological cues over prevalence data for timely cholera control. Seasonal plankton blooms, which precede cholera outbreaks by approximately 8 weeks, also offer another critical window for intervention. Phytoplankton can be monitored using remote sensing tools like chlorophyll-a concentration, while zooplankton trends can be inferred from seasonal historical data or localized sampling. Moreover, for

real-world applications, the model can be calibrated using time-series data on cholera incidence and plankton abundance. This would improve forecast accuracy, and can guide the timing of low-cost, point-of-use interventions like water filtration. Furthermore, in this study, we focused exclusively on filtration as a control measure because of its unique ability to target the zooplankton-mediated transmission pathway. However, future studies could investigate its combined effect with other intervention strategies such as implementing safe water, basic sanitation and hygiene (WASH) and providing oral vaccination. In fact, bloom forecasts could also guide reactive vaccination campaigns, targeted distribution of filtration kits, water resource management and other POU measures such as boiling or household chlorination. Hence, incorporating ecological monitoring into cholera preparedness frameworks could enable efficient and seasonally adaptive intervention strategies. Therefore, although environmental reservoirs of *V. cholera* in coastal ecosystems complicate eradication, their associated ecology can also provide an opportunity to control cholera endemicity through timely and efficient interventions.

Increased climate variability with ongoing global change and subsequent extreme weather events can influence pathogen ecology, thereby highlighting the need to integrate the same while studying disease dynamics [74]. Our model takes a first step in this direction in the context of cholera and provides qualitative insights into transmission dynamics which could be useful to inform public health policies. Despite the usefulness of our model, it has few limitations. While some studies indicate that *V. cholerae* can also associate with phytoplankton [10,75], we choose to neglect this aspect in our study. This assumption can also be justified in line with the empirical studies [13,22], where an increase in *V. cholerae* concentration has reportedly corresponded to a significant decrease in phytoplankton abundance driven by higher nutrient availability and reduced level of antibacterial metabolites. Additionally, we do not take into account the growth of *V. cholerae* [12,18] and the increased pathogen virulence [15,76] while attaching to zooplankton. Incorporating these ecological and epidemiological aspects in future cholera research could enhance our understanding of disease dynamics. The effect of other environmental factors such as nutrient cycling, temperature-dependent colonization coefficients could also add more realism to the model and could be investigated individually or in combination. The need of the hour is to shift the focus toward integrating the ecology of pathogens and their response to changing environment while predicting disease outbreaks. This could be integrated with socio-economic factors such as variability in sanitation infrastructure and human mobility affecting access to clean water and the uptake of interventions like vaccination or filtration, to provide a more holistic framework for cholera prevention.

Supporting information

S1 Text. Supplementary material. This file includes parameter definitions, proofs of positive invariance and boundedness, analysis of the phytoplankton–zooplankton model, outbreak dynamics (including sensitivity and epidemic growth analysis), and long-term dynamics (basic reproduction number and filtration efficacy impacts).
(PDF)

S1 Fig. Influence of zooplankton death rate on the basic reproduction threshold. Zooplankton death rate (d_z) increases the slope of the $\mathcal{R}_{0_{BZ}}^{out} = \mathcal{R}_0^{out}$ line and thereby decreasing region $\boxed{1}$. Here, for the solid line, $d_z = 0.06$, and for the dashed line, $d_z = 0.1$.
(TIF)

S2 Fig. Influence of σ and β_z on the epidemic growth rate. Initial epidemic growth rate (EGR) with respect to the *Vibrio*-zooplankton association rate (σ) for different zooplankton-mediated transmission rate (β_z) within region 1 in Fig 2.
(TIF)

S3 Fig. Post-peak maintenance of low-level infections. Increased zooplankton-mediated transmission (β_z) can have potentially large negative impacts on human health under a fixed bacteria-zooplankton association rate ($\sigma = 0.03$) within region 1 in Fig 2. It shortens the time to peak infection, increases the peak size, and elevates lower-level maintenance of infections during the post-peak period.
(TIF)

S4 Fig. Effect of free-living bacterial transmission on epidemic dynamics of the classical SIRB model. Effect of transmission rate via the free-living bacterial route (β) for the classical SIRB model on (A) $\mathcal{R}_0^{\text{out}}$ and attack rate, (B) cumulative infections at peak (as a proportion of the total population) and epidemic overshoot, (C) the ratio of overshoot to attack rate (ρ_{OA}), and (D) peak timing and epidemic duration in the absence of bacteria-zooplankton association ($\sigma = 0$). Intuitively, both $\mathcal{R}_0^{\text{out}}$ and attack rate increase with β. While β increases cumulative infections at peak, there exists an upper bound on the overshoot. The ratio ρ_{OA} decreases monotonically with increasing β due to the availability of fewer susceptible individuals for the overshoot (post-peak) phase. Both peak timing and epidemic duration consistently decrease as β increases.
(TIF)

S5 Fig. Z_B formation governed by available bacterial cells during zooplankton abundance. The formation of Z_B (solid and dashed blue) depends on the density of B cells (solid and dashed red) in the water column during periods of Z abundance (dotted blue line) in both unfiltered (dashed) and filtered (solid) scenarios when filtration is initiated at T_1-T_4. The shaded regions indicate the filtration periods. Filtration reduces cholera infections in two ways: first, by restricting Z_B formation through the reduction of B cell concentration during the periods Z abundance; and second, if Z_B formation cannot be avoided, by preventing its ingestion.
(TIF)

S6 Fig. Impact of filtration efficacy on cholera infection reduction. Cholera infection reduction (%) over a year under varying filtration efficacy (e_f). The solid line denotes the maximum reduction and the dotted line denotes the minimum, calculated across all possible filtration initiation timings.
(TIF)

Author contributions

Conceptualization: Biplab Maity, Swarnendu Banerjee, Abhishek Senapati, Jon Pitchford, Joydev Chattopadhyay.

Formal analysis: Biplab Maity.

Methodology: Biplab Maity, Swarnendu Banerjee, Abhishek Senapati.

Software: Biplab Maity.

Supervision: Swarnendu Banerjee, Abhishek Senapati, Joydev Chattopadhyay.

Visualization: Biplab Maity.

Writing – original draft: Biplab Maity.

Writing – review & editing: Biplab Maity, Swarnendu Banerjee, Abhishek Senapati, Jon Pitchford, Joydev Chattopadhyay.

References

1. GBD 2016 Diarrhoeal Disease Collaborators. Estimates of the global, regional, and national morbidity, mortality, and aetiologies of diarrhoea in 195 countries: a systematic analysis for the Global Burden of Disease Study 2016. Lancet Infect Dis. 2018;18(11):1211–28. https://doi.org/10.1016/S1473-3099(18)30362-1 PMID: 30243583
2. WHO. Cholera - Fact sheets. 2024. https://www.who.int/news-room/fact-sheets/detail/cholera
3. Venkatesan P. New measures to tackle the global cholera surge. Lancet Microbe. 2024;5(7):632. https://doi.org/10.1016/S2666-5247(24)00133-2 PMID: 38823412
4. WHO. Multi-country outbreak of cholera, external situation report 12-14 March 2024. 2024. https://www.who.int/publications/m/item/multi-country-outbreak-of-cholera--external-situation-report--12---14-march-
5. Ilic I, Ilic M. Global patterns of trends in cholera mortality. Trop Med Infect Dis. 2023;8(3):169. https://doi.org/10.3390/tropicalmed8030169 PMID: 36977170
6. Xu H, Zou K, Dent J, Wiens KE, Malembaka EB, Bwire G, et al. Enhanced cholera surveillance to improve vaccination campaign efficiency. Nat Med. 2024;30(4):1104–10. https://doi.org/10.1038/s41591-024-02852-8 PMID: 38443690
7. Amisu BO, Okesanya OJ, Adigun OA, Manirambona E, Ukoaka BM, Lawal OA, et al. Cholera resurgence in Africa: assessing progress, challenges, and public health response towards the 2030 global elimination target. Infez Med. 2024;32(2):148–56. https://doi.org/10.53854/liim-3202-4 PMID: 38827826
8. WHO. WHO and partners revamp war against cholera in Africa. 2022. https://www.afro.who.int/countries/united-republic-of-tanzania/news/who-and-partners-revamp-war-against-cholera-africa
9. ECDC EC for DP and C. Cholera worldwide overview. 2024. https://www.ecdc.europa.eu/en/all-topics-z/cholera/surveillance-and-disease-data/cholera-monthly
10. Islam MS, Islam MS, Mahmud ZH, Cairncross S, Clemens JD, Collins AE. Role of phytoplankton in maintaining endemicity and seasonality of cholera in Bangladesh. Trans R Soc Trop Med Hyg. 2015;109(9):572–8. https://doi.org/10.1093/trstmh/trv057 PMID: 26179653
11. de Magny GC, Mozumder PK, Grim CJ, Hasan NA, Naser MN, Alam M, et al. Role of zooplankton diversity in Vibrio cholerae population dynamics and in the incidence of cholera in the Bangladesh Sundarbans. Appl Environ Microbiol. 2011;77(17):6125–32. https://doi.org/10.1128/AEM.01472-10 PMID: 21764957
12. Huq A, Small EB, West PA, Huq MI, Rahman R, Colwell RR. Ecological relationships between Vibrio cholerae and planktonic crustacean copepods. Appl Environ Microbiol. 1983;45(1):275–83. https://doi.org/10.1128/aem.45.1.275-283.1983 PMID: 6337551
13. Huq A, Sack RB, Nizam A, Longini IM, Nair GB, Ali A, et al. Critical factors influencing the occurrence of Vibrio cholerae in the environment of Bangladesh. Appl Environ Microbiol. 2005;71(8):4645–54. https://doi.org/10.1128/AEM.71.8.4645-4654.2005 PMID: 16085859
14. Jutla AS, Akanda AS, Islam S. Satellite remote sensing of space-time plankton variability in the Bay of Bengal: connections to cholera outbreaks. Remote Sens Environ. 2012;123:196–206. https://doi.org/10.1016/j.rse.2012.03.005 PMID: 22544976
15. Vezzulli L, Pruzzo C, Huq A, Colwell RR. Environmental reservoirs of Vibrio cholerae and their role in cholera. Environ Microbiol Rep. 2010;2(1):27–33. https://doi.org/10.1111/j.1758-2229.2009.00128.x PMID: 23765995
16. Colwell RR. Global climate and infectious disease: the cholera paradigm. Science. 1996;274(5295):2025–31. https://doi.org/10.1126/science.274.5295.2025 PMID: 8953025
17. Almagro-Moreno S, Taylor RK. Cholera: environmental reservoirs and impact on disease transmission. Microbiol Spectr. 2013;1(2):10.1128/microbiolspec.OH-0003-2012. https://doi.org/10.1128/microbiolspec.OH-0003-2012 PMID: 26184966
18. Lutz C, Erken M, Noorian P, Sun S, McDougald D. Environmental reservoirs and mechanisms of persistence of Vibrio cholerae. Front Microbiol. 2013;4:375. https://doi.org/10.3389/fmicb.2013.00375 PMID: 24379807

19. Martinelli Filho JE, Lopes RM, Rivera ING, Colwell RR. Vibrio cholerae O1 detection in estuarine and coastal zooplankton. Journal of Plankton Research. 2010;33(1):51–62. https://doi.org/10.1093/plankt/fbq093
20. Lizarraga-Partida M, Mendez-Gomez E, Rivas-Montano A, Vargas-Hernandez E, Portillo-Lopez A, Gonzalez-Ramirez A. Association of Vibrio cholerae with plankton in coastal areas of Mexico. Environmental Microbiology. 2009;11(1):201–8.
21. Colwell RR, Huq A. Environmental reservoir of Vibrio cholerae. The causative agent of cholera. Ann N Y Acad Sci. 1994;740:44–54. https://doi.org/10.1111/j.1749-6632.1994.tb19852.x PMID: 7840478
22. Turner JW, Good B, Cole D, Lipp EK. Plankton composition and environmental factors contribute to Vibrio seasonality. ISME J. 2009;3(9):1082–92. https://doi.org/10.1038/ismej.2009.50 PMID: 19421235
23. Rawlings TK, Ruiz GM, Colwell RR. Association of Vibrio cholerae O1 El Tor and O139 Bengal with the Copepods Acartia tonsa and Eurytemora affinis. Appl Environ Microbiol. 2007;73(24):7926–33. https://doi.org/10.1128/AEM.01238-07 PMID: 17951440
24. Constantin de Magny G, Murtugudde R, Sapiano MRP, Nizam A, Brown CW, Busalacchi AJ, et al. Environmental signatures associated with cholera epidemics. Proc Natl Acad Sci U S A. 2008;105(46):17676–81. https://doi.org/10.1073/pnas.0809654105 PMID: 19001267
25. Heidelberg JF, Heidelberg KB, Colwell RR. Bacteria of the gamma-subclass Proteobacteria associated with zooplankton in Chesapeake Bay. Appl Environ Microbiol. 2002;68(11):5498–507. https://doi.org/10.1128/AEM.68.11.5498-5507.2002 PMID: 12406743
26. Colwell RR, Brayton P, Herrington D, Tall B, Huq A, Levine MM. Viable but non-culturable Vibrio cholerae O1 revert to a cultivable state in the human intestine. World J Microbiol Biotechnol. 1996;12(1):28–31. https://doi.org/10.1007/BF00327795 PMID: 24415083
27. Sochard MR, Wilson DF, Austin B, Colwell RR. Bacteria associated with the surface and gut of marine copepods. Appl Environ Microbiol. 1979;37(4):750–9. https://doi.org/10.1128/aem.37.4.750-759.1979 PMID: 16345368
28. Huq A, West PA, Small EB, Huq MI, Colwell RR. Influence of water temperature, salinity, and pH on survival and growth of toxigenic Vibrio cholerae serovar 01 associated with live copepods in laboratory microcosms. Appl Environ Microbiol. 1984;48(2):420–4. https://doi.org/10.1128/aem.48.2.420-424.1984 PMID: 6486784
29. Kirn TJ, Jude BA, Taylor RK. A colonization factor links Vibrio cholerae environmental survival and human infection. Nature. 2005;438(7069):863–6. https://doi.org/10.1038/nature04249 PMID: 16341015
30. Conner JG, Teschler JK, Jones CJ, Yildiz FH. Staying alive: Vibrio cholerae's cycle of environmental survival, transmission, and dissemination. Virulence mechanisms of bacterial pathogens. 2016. p. 593–633.
31. Chowdhury MA, Huq A, Xu B, Madeira FJ, Colwell RR. Effect of alum on free-living and copepod-associated Vibrio cholerae O1 and O139. Appl Environ Microbiol. 1997;63(8):3323–6. https://doi.org/10.1128/aem.63.8.3323-3326.1997 PMID: 9251224
32. Tang K, Turk V, Grossart H. Linkage between crustacean zooplankton and aquatic bacteria. Aquat Microb Ecol. 2010;61(3):261–77. https://doi.org/10.3354/ame01424
33. Perera IU, Fujiyoshi S, Nishiuchi Y, Nakai T, Maruyama F. Zooplankton act as cruise ships promoting the survival and pathogenicity of pathogenic bacteria. Microbiol Immunol. 2022;66(12):564–78. https://doi.org/10.1111/1348-0421.13029 PMID: 36128640
34. Lipp EK, Huq A, Colwell RR. Effects of global climate on infectious disease: the cholera model. Clin Microbiol Rev. 2002;15(4):757–70. https://doi.org/10.1128/CMR.15.4.757-770.2002 PMID: 12364378
35. Constantin de Magny G, Hasan NA, Roche B. How community ecology can improve our understanding of cholera dynamics. Front Microbiol. 2014;5:137. https://doi.org/10.3389/fmicb.2014.00137 PMID: 24765090
36. King AA, Ionides EL, Pascual M, Bouma MJ. Inapparent infections and cholera dynamics. Nature. 2008;454(7206):877–80. https://doi.org/10.1038/nature07084 PMID: 18704085
37. Fung IC-H. Cholera transmission dynamic models for public health practitioners. Emerg Themes Epidemiol. 2014;11(1):1. https://doi.org/10.1186/1742-7622-11-1 PMID: 24520853
38. Mukandavire Z, Liao S, Wang J, Gaff H, Smith DL, Morris JG Jr. Estimating the reproductive numbers for the 2008-2009 cholera outbreaks in Zimbabwe. Proc Natl Acad Sci U S A. 2011;108(21):8767–72. https://doi.org/10.1073/pnas.1019712108 PMID: 21518855
39. Miller Neilan RL, Schaefer E, Gaff H, Fister KR, Lenhart S. Modeling optimal intervention strategies for cholera. Bull Math Biol. 2010;72(8):2004–18. https://doi.org/10.1007/s11538-010-9521-8 PMID: 20204710

40. Andrews JR, Basu S. Transmission dynamics and control of cholera in Haiti: an epidemic model. Lancet. 2011;377(9773):1248–55. https://doi.org/10.1016/S0140-6736(11)60273-0 PMID: 21414658
41. Maity B, Saha B, Ghosh I, Chattopadhyay J. Model-based estimation of expected time to cholera extinction in Lusaka, Zambia. Bull Math Biol. 2023;85(7):55. https://doi.org/10.1007/s11538-023-01149-0 PMID: 37208444
42. Islam MS, Drasar BS, Sack RB. Probable role of blue-green algae in maintaining endemicity and seasonality of cholera in Bangladesh: a hypothesis. J Diarrhoeal Dis Res. 1994;12(4):245–56. PMID: 7751564
43. Kolaye G, Bowong S, Houe R, Aziz-Alaoui MA, Cadivel M. Mathematical assessment of the role of environmental factors on the dynamical transmission of cholera. Communications in Nonlinear Science and Numerical Simulation. 2019;67:203–22.
44. Codeço CT. Endemic and epidemic dynamics of cholera: the role of the aquatic reservoir. BMC Infect Dis. 2001;1:1.https://doi.org/10.1186/1471-2334-1-1 PMID: 11208258
45. Righetto L, Casagrandi R, Bertuzzo E, Mari L, Gatto M, Rodriguez-Iturbe I, et al. The role of aquatic reservoir fluctuations in long-term cholera patterns. Epidemics. 2012;4(1):33–42. https://doi.org/10.1016/j.epidem.2011.11.002 PMID: 22325012
46. Rosenzweig ML. Paradox of enrichment: destabilization of exploitation ecosystems in ecological time. Science. 1971;171(3969):385–7. https://doi.org/10.1126/science.171.3969.385 PMID: 5538935
47. Hartley DM, Morris JG Jr, Smith DL. Hyperinfectivity: a critical element in the ability of V. cholerae to cause epidemics?. PLoS Med. 2006;3(1):e7. https://doi.org/10.1371/journal.pmed.0030007 PMID: 16318414
48. Sanches RP, Ferreira CP, Kraenkel RA. The role of immunity and seasonality in cholera epidemics. Bull Math Biol. 2011;73(12):2916–31. https://doi.org/10.1007/s11538-011-9652-6 PMID: 21468779
49. Dimitrov DT, Troeger C, Halloran ME, Longini IM, Chao DL. Comparative effectiveness of different strategies of oral cholera vaccination in bangladesh: a modeling study. PLoS Negl Trop Dis. 2014;8(12):e3343. https://doi.org/10.1371/journal.pntd.0003343 PMID: 25473851
50. Miller Neilan RL, Schaefer E, Gaff H, Fister KR, Lenhart S. Modeling optimal intervention strategies for cholera. Bull Math Biol. 2010;72(8):2004–18. https://doi.org/10.1007/s11538-010-9521-8 PMID: 20204710
51. Keeling MJ, Rohani P. Modeling infectious diseases in humans and animals. Princeton University Press; 2008.
52. Martcheva M. An introduction to mathematical epidemiology. Springer; 2015.
53. Koelle K, Rodó X, Pascual M, Yunus M, Mostafa G. Refractory periods and climate forcing in cholera dynamics. Nature. 2005;436(7051):696–700. https://doi.org/10.1038/nature03820 PMID: 16079845
54. Jensen MA, Faruque SM, Mekalanos JJ, Levin BR. Modeling the role of bacteriophage in the control of cholera outbreaks. Proc Natl Acad Sci U S A. 2006;103(12):4652–7. https://doi.org/10.1073/pnas.0600166103 PMID: 16537404
55. Scheffer M. Fish and nutrients interplay determines algal biomass: a minimal model. Oikos. 1991;62(3):271. https://doi.org/10.2307/3545491
56. Silva AJ da, Melo PAM de C, Neumann-Leitão S, de Melo Júnior M. Non-predatory mortality of planktonic copepods in a reef area influenced by estuarine plume. Mar Environ Res. 2020;159:105024. https://doi.org/10.1016/j.marenvres.2020.105024 PMID: 32662423
57. Hirst A, Kiørboe T. Mortality of marine planktonic copepods: global rates and patterns. Mar Ecol Prog Ser. 2002;230:195–209. https://doi.org/10.3354/meps230195
58. Di Capua I, Mazzocchi MG. Non-predatory mortality in Mediterranean coastal copepods. Mar Biol. 2017;164(10). https://doi.org/10.1007/s00227-017-3212-z
59. Freund JA, Mieruch S, Scholze B, Wiltshire K, Feudel U. Bloom dynamics in a seasonally forced phytoplankton–zooplankton model: Trigger mechanisms and timing effects. Ecological Complexity. 2006;3(2):129–39. https://doi.org/10.1016/j.ecocom.2005.11.001
60. Shackleton D, Memon FA, Nichols G, Phalkey R, Chen AS. Mechanisms of cholera transmission via environment in India and Bangladesh: state of the science review. Rev Environ Health. 2023;39(2):313–29. https://doi.org/10.1515/reveh-2022-0201 PMID: 36639850
61. Handel A, Longini IM Jr, Antia R. What is the best control strategy for multiple infectious disease outbreaks?. Proc Biol Sci. 2007;274(1611):833–7. https://doi.org/10.1098/rspb.2006.0015 PMID: 17251095

62. Nguyen MM, Freedman AS, Ozbay SA, Levin SA. Fundamental bound on epidemic overshoot in the SIR model. J R Soc Interface. 2023;20(209):20230322. https://doi.org/10.1098/rsif.2023.0322 PMID: 38053384
63. D'Silva MS, Anil AC, Naik RK, D'Costa PM. Algal blooms: a perspective from the coasts of India. Natural Hazards. 2012;63:1225–53.
64. Baracchini T, King AA, Bouma MJ, Rodó X, Bertuzzo E, Pascual M. Seasonality in cholera dynamics: a rainfall-driven model explains the wide range of patterns in endemic areas. Advances in Water Resources. 2017;108:357–66. https://doi.org/10.1016/j.advwatres.2016.11.012
65. Huq A, Xu B, Chowdhury MA, Islam MS, Montilla R, Colwell RR. A simple filtration method to remove plankton-associated Vibrio cholerae in raw water supplies in developing countries. Appl Environ Microbiol. 1996;62(7):2508–12. https://doi.org/10.1128/aem.62.7.2508-2512.1996 PMID: 8779590
66. Colwell RR, Huq A, Islam MS, Aziz KMA, Yunus M, Khan NH, et al. Reduction of cholera in Bangladeshi villages by simple filtration. Proc Natl Acad Sci U S A. 2003;100(3):1051–5. https://doi.org/10.1073/pnas.0237386100 PMID: 12529505
67. Huq A, Yunus M, Sohel SS, Bhuiya A, Emch M, Luby SP, et al. Simple sari cloth filtration of water is sustainable and continues to protect villagers from cholera in Matlab, Bangladesh. mBio. 2010;1(1):e00034-10. https://doi.org/10.1128/mBio.00034-10 PMID: 20689750
68. Enserink M. In the cradle of cholera. Science. 2025;387(6734):572–7. https://doi.org/10.1126/science.adw4664 PMID: 39913596
69. Sobsey MD, Stauber CE, Casanova LM, Brown JM, Elliott MA. Point of use household drinking water filtration: a practical, effective solution for providing sustained access to safe drinking water in the developing world. Environ Sci Technol. 2008;42(12):4261–7. https://doi.org/10.1021/es702746n PMID: 18605542
70. Taylor DL, Kahawita TM, Cairncross S, Ensink JHJ. The impact of water, sanitation and hygiene interventions to control Cholera: a systematic review. PLoS One. 2015;10(8):e0135676. https://doi.org/10.1371/journal.pone.0135676 PMID: 26284367
71. Fewtrell L, Kaufmann RB, Kay D, Enanoria W, Haller L, Colford JM Jr. Water, sanitation, and hygiene interventions to reduce diarrhoea in less developed countries: a systematic review and meta-analysis. Lancet Infect Dis. 2005;5(1):42–52. https://doi.org/10.1016/S1473-3099(04)01253-8 PMID: 15620560
72. Tien JH, Earn DJD. Multiple transmission pathways and disease dynamics in a waterborne pathogen model. Bull Math Biol. 2010;72(6):1506–33. https://doi.org/10.1007/s11538-010-9507-6 PMID: 20143271
73. Sack DA, Debes AK, Ateudjieu J, Bwire G, Ali M, Ngwa MC, et al. Contrasting epidemiology of cholera in Bangladesh and Africa. J Infect Dis. 2021;224(12 Suppl 2):S701–9. https://doi.org/10.1093/infdis/jiab440 PMID: 34549788
74. Brumfield KD, Usmani M, Long DM, Lupari HA, Pope RK, Jutla AS, et al. Climate change and Vibrio: environmental determinants for predictive risk assessment. Proc Natl Acad Sci U S A. 2025;122(33):e2420423122. https://doi.org/10.1073/pnas.2420423122 PMID: 40789031
75. Seeligmann CT, Mirande V, Tracanna BC, Silva C, Aulet O, Cecilia M, et al. Phytoplankton-linked viable non-culturable Vibrio cholerae O1 (VNC) from rivers in Tucuman, Argentina. Journal of Plankton Research. 2008;30(4):367–77. https://doi.org/10.1093/plankt/fbn008
76. Walther BA, Ewald PW. Pathogen survival in the external environment and the evolution of virulence. Biol Rev Camb Philos Soc. 2004;79(4):849–69. https://doi.org/10.1017/s1464793104006475 PMID: 15682873